Journal of Sound and Vibration (1998) **210**(4), 431–439

INCREASING THE MAXIMUM STABLE ROTATION SPEED OF A CIRCULAR DISK USING SPEED DEPENDENT CLAMPING

A. A. Renshaw

Department of Mechanical Engineering, Columbia University, New York, 10027, U.S.A.

(*Received* 16 *September* 1996, *and in final form* 24 *February* 1997)

In this paper a stress induction method is examined that can be used to increase the operational speed range of rotating disks such as industrial circular saws and computer disk drives. In this method, stresses are generated in the disk by producing displacements or tractions at the inner radius of the disk that are proportional to the square of the rotation speed; as might be achieved, for example, by allowing freely sliding, centripetally accelerating, concentrated masses to rest along the inner radius of the disk. While traditional stress induction techniques can raise the maximum rotation speed by 30–40%, the technique proposed here can *double* the maximum speed for hydrodynamically uncoupled disks (circular saws and hard disk drives) and can increase the maximum speed of disks with substantial hydrodynamic coupling (floppy disks) by an *order of magnitude*. These increases and the optimal stress induction parameters are studied in detail here.

1. INTRODUCTION

Thin, high speed rotating disks are the principal mechanical components of industrial circular saws and computer disk drives. In each of these technologies, thinner disks and faster rotation are desirable either to increase production or reduce data acquisition times. However, the useful operational speed range and disk thinness in these devices are usually limited by a critical speed phenomenon, in which the propagation of a circumferentially travelling wave is equal and opposite the rotation of the disk [1–6]. Neither industrial saws nor computer disk drives can tolerate the large transverse deflections that occur near the critical speed, and, consequently, these devices generally operate at a fraction of the lowest critical speed [7].

For many decades, the saw industry has induced in-plane residual stresses in saw blades to counteract the thermal stresses that arise at the periphery of the saw and to increase the saw's operational speed range [8, 9]. These residual stresses are normally produced using a technique called "roll-tensioning", in which a thin, circumferential ring of the disk is plastically deformed by repeatedly rolling it between two loaded wheels [4, 10–14]. Other stress induction methods have also been proposed [15–17]. Although potentially beneficial, residual stresses are generally not induced in computer disk drives because of their sensitivity to disk integrity and processing.

In this paper a new stress induction method is examined that can be used in both circular saws and computer disk drives. In this method, stresses are generated in the disk by the central clamp, which is designed to produce tractions or in-plane displacements at the inner radius that are proportional to the square of the rotation speed; as might be achieved, for example, by allowing freely sliding, centripetally accelerating, concentrated massses to rest

0022–460X/98/090431 + 09 $25.00/0/sv970994

along the inner radius of the disk. This might be possible using a scalloped spline to drive the disk, since a clamp attached to the spline could prevent transverse motion of the disk without constraining the radial motion. Alternatively, the drive shaft could be split so that it flies radially outwards during rotation.

Regulating the induced stress with speed dependent boundary tractions or displacements has two advantages: first, the technique can be applied without affecting the integrity of the disk, which would permit its use in computer disk drives; and, second, significantly higher rotation speeds are possible than produced by other techniques. This occurs because the induced stresses are generated while the disk is rotating, and the destabilizing effects of the induced stress can be counteracted by tensile centripetal stress.

In conventional roll-testing, the critical speed can be raised by 30–40% at most before the residual stresses cause instability [14]: the technique described here can *double* critical speed for hard rotating disk such as circular saws and hard disk drives, and can increase the critical speed in flexible, hydrodynamically coupled, rotating disks such as floppy disk drives by an *order of magnitude*. In this paper a detailed analysis is provided of the increase in critical speed for both hard and flexible rotating disks using the proposed stress induction technique. Optimal traction and displacement parameters and practical considerations are also discussed.

2. THE HARD DISK CASE: A DISK DECOUPLED FROM THE SURROUNDING MEDIUM

A thin, axisymmetric, circular disk clamped at inner radius R_i and free at outer radius R_o spins about its axis of symmetry at a constant angular speed Ω^*. The disk is of uniform thickness h, density ρ (mass per unit volume), Young's modulus E, and Poisson ratio v. The polar co-ordinates (R, θ) are fixed in the staionary frame of reference, with the centre of the disk at the origin. The in-plane, radial displacement of the disk is U_r, the transverse displacement of the disk is W, and the in-plane, axisymmetric stresses σ_r^* and σ_θ^* are the sums of the centrifugal and boundary-induced stresses. Dimensionless variables describing the disk are defined by

$$r = R/R_o, \qquad w = W/h, \qquad \Omega = \Omega^*\sqrt{\rho h R_o^4/D},$$
$$u_r = U_r R_o/h^2, \qquad \sigma_r = \sigma_r^* h R_o^2/D, \qquad \sigma_\theta = \sigma_\theta^* h R_o^2/D, \tag{1}$$

where $D = Eh^3/[12(1 - v^2)]$. The clamping ratio $\kappa = R_i/R_o$.

In this section we consider hard disks such as industrial circular saws and hard computer memory drives, the motions of which are nominally decoupled from the motion of the surrounding medium. The transverse vibration and stability of such disks can be modelled using clasical Kirchhoff plate theory with in-plane stresses [4, 5, 18]. For that model, the maximum stable rotation speed $\Omega_{H\text{-}max}$ is given by the maximum value of Ω for which the functional J_H is positive definite [6]:

$$J_H[w] = U[w] - \tfrac{1}{2}\int \Omega^2 w^2{}_{,\theta}\, \mathrm{d}A. \tag{2}$$

U is the potential energy of the disk:

$$U[w] = \tfrac{1}{2}\int (\nabla^2 w)^2 - 2(1 - v)[w_{,rr}(w_{,r}/r + w_{,\theta\theta}/r^2) - [(w_{,\theta}/r)_{,r}]^2] + \sigma_r w_{,r}^2 + \sigma_\theta w_{,\theta}^2/r^2\, \mathrm{d}A. \tag{3}$$

A comma indicates partial differentiation, and dA is the different planar area of the disk. Admissible functions for J_H and U satisfy clamped–free boundary conditions:

$$w = 0 \quad \text{and} \quad w_{,r} = 0 \quad \text{at} \quad r = \kappa, \qquad w_{,rr} + \nu(w_{,r}/r + w_{,\theta\theta}/r^2) = 0 \quad \text{at} \quad r = 1,$$

$$(\nabla^2 w)_{,r} + (1 - \nu)(w_{,r\theta\theta}/r^2 - w_{,\theta\theta}/r^3) = 0 \quad \text{at} \quad r = 1. \tag{4}$$

∇^2 is the Laplacian operator.

The clamp of the disk is designed to produce the speed dependent traction at the inner boundary:

$$\sigma_r = -m\Omega^2 \quad \text{at} \quad r = \kappa. \tag{5}$$

The outer edge of the disk is free:

$$\sigma_r = 0 \quad \text{at} \quad r = 1; \tag{6}$$

m is a constant that could represent the total dimensionless added mass, assumed to be concentrated in a line around the inner radius $r = \kappa$, although the traction could be produced in some other manner such as electromagnetically. This mass would produce the specified traction. $m = 0$ represents an annular disk with no traction at $r = \kappa$ which is often used to model rotating disk systems [19]. The axisymmetric solutions of the generalized plane stress equations of linear elasticity with a centripetal body force and single valued displacements that satisfy equations (5) and (6) are

$$\sigma_r = \Omega^2[c_1/r^2 + c_2 + c_3 r^2], \qquad \sigma_\theta = \Omega^2[-c_1/r^2 + c_2 + c_4 r^2], \tag{7}$$

where

$$c_1 = -(3 + \nu)\kappa^2/8 - m\kappa^2/(1 - \kappa^2), \qquad c_2 = (1 + \kappa^2)(3 + \nu)/8 + m\kappa^2/(1 - \kappa^2),$$

$$c_3 = -(3 + \nu)/8, \qquad c_4 = -(1 + 3\nu)/8.$$

Since J_H is separable in θ, $\Omega_{H\text{-}max}$ can be determined numerically by solving the symmetric eigenvalue problem for Ω, defining the extrema of J_H for $n = 0, 1, 2, \ldots$ using the substitution $w = u(r)\cos(n\theta)$. In Figure 1 are shown plots of $\Omega_{H\text{-}max}$ and the number of nodal diameters, n, in the non-definite eigenfunction as a function of κ for $m = 0$, 1 and 2. These values were determined using the Galerkin method with six orthonormal, Chebyshev polynomials defining $u(r)$. As few as three polynomials were sufficient to give convergence within 1% of the reported values [6]. The search was carried out from $n = 0$ to $n = 10$. The results show that $\Omega_{H\text{-}max}$ can be approximately doubled from its value when $m = 0$ by an appropriate choice of m. For $\kappa = 0{\cdot}35$, increasing m from 0 to 1 increases $\Omega_{H\text{-}max}$ from 7·21 to 14·5, an increase of 101%. For $\kappa = 0{\cdot}24$, increasing m from 0 to 2 increases $\Omega_{H\text{-}max}$ from 5·91 to 10·6, an increase of 79%. When $m = 0$, the non-definite eigenfunction has two or more nodal diameters [20], but the peak increase in $\Omega_{H\text{-}max}$ occurs at the transition between a non-definite eigenfunction with non-zero nodal diameters and one with zero nodal diameters. This causes the cusp-like behavior to the curves, since each side of the peak is determined by a different eigensolution.

In Figure 2 are shown plots of m_{opt}, the value of m that maximizes $\Omega_{H\text{-}max}$, and the corresponding value of $\Omega_{H\text{-}max}$ as a function of κ. Also shown is the allowable variation in m_{opt} for which $\Omega_{H\text{-}max}$ remains within 90% of its maximum value. The results verify that $\Omega_{H\text{-}max}$ can be approximately doubled for all values of κ with an appropriate choice of m. Furthermore, a 10% variation in m from its optimal value produces about a 10% decrease in $\Omega_{H\text{-}max}$.

For most current hard disk designs, m_{opt} is relatively large. Consider the industrial circular saw studied by D'Angelo and Mote [19], for which $R_o = 0{\cdot}178$ m, $R_i = 0{\cdot}0534$ m, $h = 0{\cdot}775$ mm and $\rho = 7700$ kg/m^3. The total mass of the disk is 0·54 kg. For $\kappa = 0{\cdot}3$, $m_{opt} = 1{\cdot}35$, giving $\Omega_{H\text{-}max} = 12{\cdot}6$, an increase of 90% over $m = 0$. The total mass required at the inner edge of the disk, $2\pi m\rho h R_o^2$, is 1·6 kg, or three times the mass of the disk. Similarly, for a 5 inch disk in a hard disk drive, $R_o = 65$ mm, $R_i = 19{\cdot}5$ mm, $h = 1{\cdot}3$ mm and $\rho = 2800$ kg/m^3 [6]. In this case, the total mass of the disk is 44 g, while the total mass required at the inner edge is 130 g. In Figure 3 is shown the mass ratio, $2\,m_{opt}/(1-\kappa^2)$, the ratio of the total clamping mass required to optimally increase $\Omega_{H\text{-}max}$ to the total mass of the disk, as a function of κ. As κ increases, this ratio decreases monotonically to values that are more easily achieved in practice. For example, if κ is increased to 0·5, then $m_{opt} = 0{\cdot}42$. The mass of the equivalent circular saw then becomes 0·45 kg, while the clamping mass is only 0·50 kg.

3. THE FLOPPY DISK CASE: A DISK COUPLED TO THE SURROUNDING MEDIUM

In this section we consider flexible spinning disks such as computer floppy disks, the motions of which are strongly coupled to the motion of the surrounding medium. We restrict ourselves to the case in which the disk is enclosed in a housing similar to that of a floppy disk, which is sealed to prevent radial flow at the outer edge of the disk and the clearance of which is sufficiently small to justifiy modelling the air flow using hydrodynamic lubrication theory. The hydrodynamic coupling in a floppy disk is essential to its design, and the floppy disk would not function properly in its absence [6, 21]. The

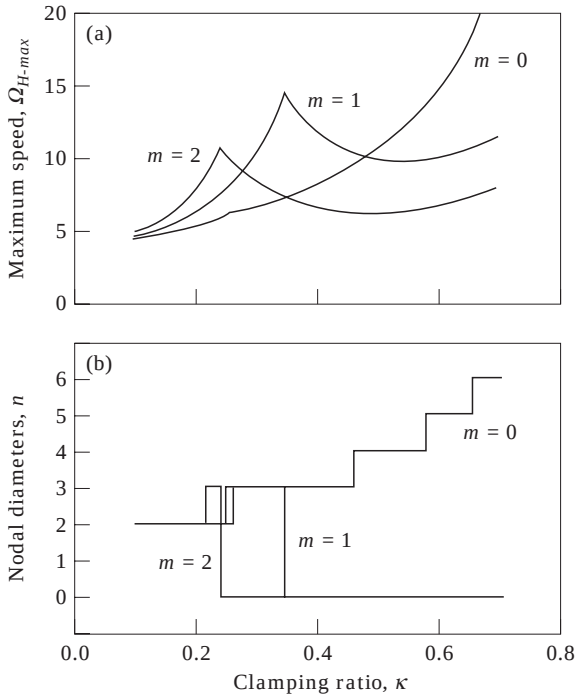

Figure 1. (a) The hard disk critical speed, $\Omega_{H\text{-}max}$, and (b) the number of nodal diameters in the critical eigensolution, n, as functions of the clamping ratio, κ, for $m = 0$, 1 and 2.

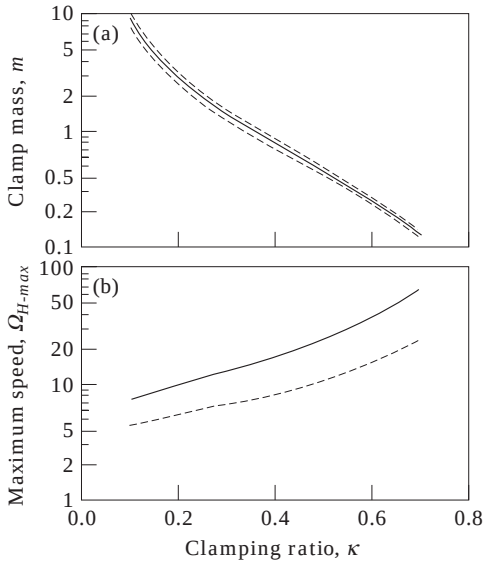

Figure 2. (a) The optimal value of m, m_{opt}, and (b) the resulting hard disk critical speed, $\Omega_{H\text{-}max}$, as functions of κ. In (a) the dashed lines indicate the variation in m that produces 90% of the optimal increase in rotation speed. In (b): ——, $m=m_{opt}$; ---, $m=0$.

stability of hydrodynamically coupled rotating disks is also fundamentally different from that of hard disks [6].

For this model, the maximum stable rotation speed $\Omega_{F\text{-}max}$ is the maximum value of Ω for which the functional J_F is positive definite [6]:

$$J_F[w] = U[w] - \tfrac{1}{2}\int \{\Omega^2 w_{,\theta}^2/4\}\, \mathrm{d}A. \tag{9}$$

Admissible w still satisfy equation (4).

Because of the increased flexibility of the disk, the traction boundary condition of the previous section, equation (5), is modified to the mathematically equivalent but physically more relevant speed dependent displacement boundary condition

$$u_r = \mathrm{d}\Omega^2 \quad \text{at} \quad r = \kappa. \tag{10}$$

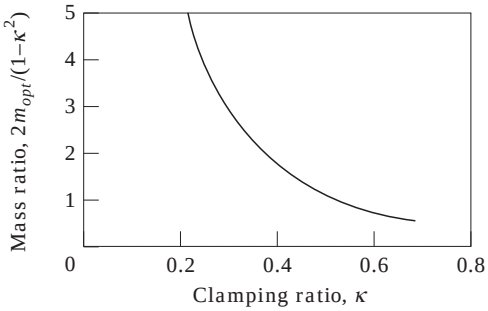

Figure 3. The ratio of the total clamping mass to optimally increase $\Omega_{H\text{-}max}$ to the total disk mass as a function of κ.

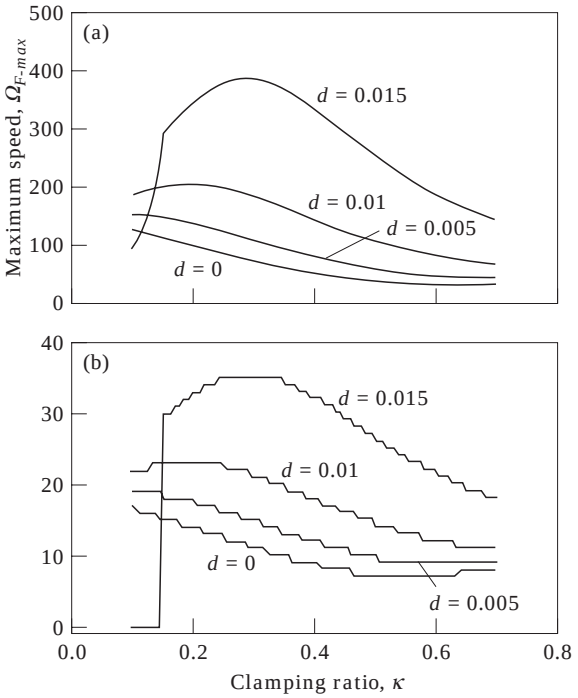

Figure 4. (a) The floppy disk critical speed, $\Omega_{F\text{-}max}$, and (b) the number of nodal diameters in the critical eigensolution, n, as functions of the clamping ratio, κ, for $d = 0$, 0·005, 0·01 and 0·015.

The stress field is still given by equation (7) and the radial displacement is

$$u_r = \frac{\Omega^2}{12(1-\nu^2)}[-c_1(1+\nu)/r + c_2(1-\nu)r - (1-\nu^2)r^3/8]. \tag{11}$$

The constants c_1 and c_2 are given by

$$c_1 = \frac{\kappa^2(1-\nu)[3+\nu-(1+\nu)\kappa^2]}{8[1+\nu+(1-\nu)\kappa^2]} - \frac{12d\kappa(1-\nu^2)}{[1+\nu+(1-\nu)\kappa^2]},$$

$$c_2 = \frac{(1+\nu)[3+\nu+(1-\nu)\kappa^4]}{8[1+\nu+(1-\nu)\kappa^2]} + \frac{12d\kappa(1-\nu^2)}{[1+\nu+(1-\nu)\kappa^2]}; \tag{12}$$

c_3 and c_4 are the same as in equation (8).

In Figure 4 are shown plots of $\Omega_{F\text{-}max}$ and the number of nodal diameters, n, in the non-definite eigenfunction as a function of κ for $d = 0$, 0·005, 0·01 and 0·015. The numerical procedure used was identical to that of the previous section, except that 13 radial polynomials were used instead of six, and the search was carried out from $n = 0$ to $n = 40$. Ten polynomials were required to give convergence within 1% of the values reported here. In Figure 5 is shown the same data as Figure 4 for $d = 0{\cdot}02$, but with substantially different scales. In Figure 5, the search was carried out from $n = 0$ to $n = 150$, using 17 radial polynomials in order to preserve the accuracy of the solution. Because of the hydrodynamic coupling, the floppy disk base case with $d = 0$ has critical speeds that are approximately two orders of magnitude greater than the uncoupled, hard disk base case with $m = 0$. Small increases in d can raise the hydrodynamically coupled critical speed substantially above the already elevated $d = 0$ levels, and it appears from Figure 5 that order of magnitude increases are possible with a proper choice of d.

These numerical solutions require a large number of trial functions to converge, and many of these solutions have a large number of nodal diameters. Eigensolutions with large numbers of nodal diameters are common in floppy disk analyses because of the mathematical structure of the model [21]. Floppy disks can also undergo large transverse deflections which require non-linear modelling and could limit the usefulness of these linear results [22].

The increase shown in Figures 4 and 5 correspond to in-plane radial displacements at the clamp on the order of the disk thickness. For example, consider a typical floppy disk with $h = 0{\cdot}05$ mm and $R_o = 42{\cdot}5$ mm. The ratio of the in-plane displacement at the clamp over the thickness is $U_r/h = d\Omega^2 h/R_o$. For $\kappa = 0{\cdot}31$ and $d = 0{\cdot}005$, $0{\cdot}01$ and $0{\cdot}015$, $\Omega_{F\text{-}max} = 69{\cdot}8$, 106, 178 and 383. The corresponding displacement ratios are $U_r/h = 0$, $0{\cdot}066$, $0{\cdot}37$ and $2{\cdot}6$.

4. PRACTICAL CONSIDERATIONS

The traction and displacement boundary conditions (5) and (10) are formally equivalent with

$$m = \frac{(1-\kappa^2)[48d(1-\nu^2) - (3+3\nu+\nu^2)\kappa + (1+\nu)\kappa^3]}{4\kappa[1+\nu+(1-\nu)\kappa^2]}, \tag{13}$$

Hence the results in Figures 4 and 5 can be directly translated into values of m instead of d and vice versa. For example, $m = 0$, $\nu = 0{\cdot}3$ and $\kappa = 0{\cdot}3$ corresponds to $d = 0{\cdot}025$. Hence a floppy disk with traction-free inner boundary conditions has a critical speed over four orders of magnitude higher than the same rotating disk in the absence of hydrodynamic coupling and two orders of magnitude higher than the same rotating disk with hydrodynamic coupling but vanishing in-plane displacements. There is a significant advantage to designing floppy disks with in-plane flexibility at the central clamp. It may

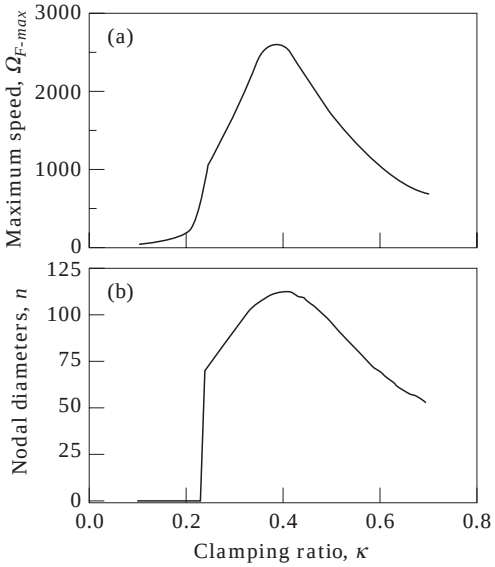

Figure 5. (a) The floppy disk critical speed, $\Omega_{F\text{-}max}$, and (b) the number of nodal diameters in the critical eigensolution, n, as functions of clamping ratio, κ, for $d = 0{\cdot}02$. Note the change in scale from Figure 4.

also be advantageous to apply additional radial tractions to floppy disk inner radii to increase d and achieve further increase in the maximum speed.

The dual traction and displacement formulations are presented here to underscore the physical differences in the two types of clamping. In practice, all clamps involve a combination of traction and displacement control involving stiction and transverse clamping pressure which is impossible to predict *a priori*, and which can be a non-linear function of the disk rotation history [19]. These difficulties hinder the design of the proposed stress induction clamp for a specific value of m or d. However, although boundary conditions proportional to Ω^2 may be achieved using rotating mass, the primary motivation for choosing these particular boundary conditions instead of any other speed dependent function was numerical convenience: for the choice of Ω^2, the maximum rotation speed is the solution of a symmetric eigenvalue problem. In practice, any choice of speed dependent boundary conditions that generated low levels of stress in the stationary or slowly rotating disk and high levels of stress in the high speed rotating disk would produce similar results, since the centripetal stresses could still counteract the destabilizing effects of the induced stress. A closed loop control system that varied the magnitude of in-plane force or displacement as a function of the disk vibration and rotation speed could also be used [16]. Such a control system could generate conditions corresponding to optimal values of m or d without having to predict the in-plane stiction, the transverse clamping force or the actual speed dependence.

Although inappropriate for computer disk drives, saw blades frequently have radial slots cut into the periphery of the blade [23]. These slots reduce the compressive, thermally induced, hoop stress that occurs along the periphery during the cutting process. In the absence of these slots, the compressive stresses can lower the maximum rotation speed. Most stress-induction techniques for raising critical speed, including the one proposed here, rely on the generation of tensile hoop stress in the periphery of the disk. Slots and other disk modifications [17, 24] that limit the tensile hoop stress generated at the periphery of the disk may be counter-productive when used with stress induction methods.

5. CONCLUSIONS

A novel stress induction method is proposed for increasing the operational speed range of rotating disks such as industrial circular saws and computer disk drives. The method involves producing a traction or displacement at the inner radius of the disk that is proportional to the square of the rotation speed. While traditional stress induction methods can increase the maximum speed of rotational disks by 30–40%, the method described here can double the maximum speed for disks with little hydrodynamic coupling, and can increase the maximum speed of hydrodynamically coupled disks by an order of magnitude.

REFERENCES

1. H. Lamb and R. V. Southwell 1921 *Proceedings of the Royal Society of London* **A99**, 272–280. The vibrations of a spinning disk.
2. R. V. Southwell 1922 *Proceedings of the Royal Society of London* **101**, 133–153. On the free transverse vibrations of a uniform circular disc clamped at its centre; and on the effects of rotation.
3. S. A. Tobias and R. N. Arnold 1957 *Proceedings of the Institution of Mechanical Engineers* **171**, 669–690. The influence of dynamic imperfections on the vibration of rotating disks.
4. C. C. Mote, Jr. 1965 *Journal of Engineering for Industry* **87**, 285–264. Free vibration of initially stressed circular disks.

5. W. D. Iwan and T. L. Moeller 1976 *Journal of Applied Mechanics* **43**, 485–490. The stability of a spinning elastic disk with a transverse load system.
6. A. A. Renshaw *Journal of Applied Mechanics*, (accepted). Critical speed for floppy disks.
7. C. D'Angelo III and C. D. Mote, Jr. 1993 *Journal of Sound and Vibration* **168**, 15–30. Aerodynamically excited vibration and flutter of a thin disk rotating at supercritical speed.
8. E. Lindholm 1953 *Arkiv for Fysik* **6**, 223–242. The vibrations and bending of pre-stressed circular plates.
9. C. C. Mote, Jr. and R. Szymani 1978 *The Shock and Vibration Digest* **10**, 15–30. Circular saw vibration research.
10. D. S. Dugdale 1963 *International Journal of Engineering Sciences* **1**, 89–100. Effect of internal stress on the flexural stiffness of discs.
11. D. S. Dugdale 1966 *International Journal of Production Research* **4**, 237–248. Theory of circular saw tensioning.
12. C. D. Mote, Jr. and L. T. Nieh 1973 *Wood Fiber* **5**, 160–169. On the foundations of circular saw stability theory.
13. J. F. Carlin, F. C. Appl, H. C. Bridwell and R. P. DuBois 1975 *Journal of Engineering for Industry* **97**, 37–48. Effects of tensioning on buckling and vibration of circular saw blades.
14. G. S. Schajer and C. D. Mote, Jr. 1983 *Wood Science and Technology* **17**, 287–302. Analysis of roll tensioning and its influence on circular saw stability.
15. C. D. Mote, Jr. 1967 *Journal of Engineering for Industry* **89**, 611–618. Natural frequencies in annuli with induced thermal membrane stresses.
16. C. D. Mote, Jr. and A. Rahimi 1984 *Journal of Dynamic Systems*, *Measurement and Control* **106**, 123–128. Real time vibration control of rotating circular plates by temperature control and system identification.
17. R. G. Parker and C. D. Mote, Jr. 1991 *Journal of Sound and Vibration* **145**, 95–110. Tuning of the natural frequency spectrum of a circular plate by in plane stress.
18. J. L. Nowinski 1964 *Journal of Applied Mechanics* **31**, 72–78. Nonlinear transverse vibrations of a spinning disk.
19. C. D. D'Angelo III and C. D. Mote, Jr. 1993 *Journal of Sound and Vibration* **168**, 1–14. Natural frequencies of a thin disk, clamped by thick collars with friction at the contacting surfaces, spinning at high rotation.
20. A. A. Renshaw and C. D. Mote, Jr. 1993 *Journal of Applied Mechanics* **59**, 687–688. Absence of one nodal diameter critical speed modes in an axisymmetric rotating disk.
21. R. C. Benson and D. B. Bogy 1978 *Journal of Applied Mechanics* **45**, 636–642. Deflection of a very flexible spinning disk due to a stationary transverse load.
22. A. A. Renshaw and C. D. Mote, Jr. 1995 *Journal of Sound and Vibration* **183**, 309–326. A perturbation solution for the flexible rotating disk: nonlinear equilibrium and stability under transverse loading.
23. R. C. Yu and C. D. Mote, Jr. 1987 *Journal of Sound and Vibration* **199**, 409–427. Vibration and parametric excitation in asymmetric circular plates under moving loads.
24. C. D. Mote, Jr. 1972 *Journal of Dynamic Systems*, *Measurement*, *and Control* **94**, 64–70. Stability control analysis of rotating plates by finite element: emphasis on slots and holes.